AD-A176 621 PHASE PATTERN OF PHASED ARRAY ELEMENT(U) NAVAL RESEARCH LAB WASHINGTON DC J B RAO ET AL. 31 DEC 86 NRL-MR-5888 1/1

UNCLASSIFIED F/G 20/14 NL

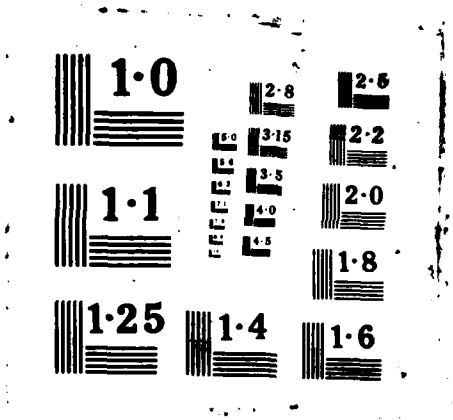
1·0
1·1
1·25
1·4
1·6
1·8
2·0
2·2
2·5
2·8
3·15
3·5
4·0
4·5

# Phase Pattern of Phased Array Element

J. B. L. RAO AND T. C. CHESTON

*Electromagnetics Branch*
*Radar Division*

SECURITY CLASSIFICATION OF THIS PAGE

# REPORT DOCUMENTATION PAGE

| | |
|---|---|
| 1a. REPORT SECURITY CLASSIFICATION<br>UNCLASSIFIED | 1b. RESTRICTIVE MARKINGS |
| 2a. SECURITY CLASSIFICATION AUTHORITY | 3. DISTRIBUTION/AVAILABILITY OF REPORT<br>Approved for public release; distribution unlimited. |
| 2b. DECLASSIFICATION/DOWNGRADING SCHEDULE | |
| 4. PERFORMING ORGANIZATION REPORT NUMBER(S)<br>NRL Memorandum Report 5888 | 5. MONITORING ORGANIZATION REPORT NUMBER(S) |
| 6a. NAME OF PERFORMING ORGANIZATION<br>Naval Research Laboratory<br>6b. OFFICE SYMBOL (If applicable)<br>Code 5372 | 7a. NAME OF MONITORING ORGANIZATION |
| 6c. ADDRESS (City, State, and ZIP Code)<br>Washington, DC 20375-5000 | 7b. ADDRESS (City, State, and ZIP Code) |
| 8a. NAME OF FUNDING/SPONSORING ORGANIZATION<br>Chief of Naval Research<br>8b. OFFICE SYMBOL (If applicable) | 9. PROCUREMENT INSTRUMENT IDENTIFICATION NUMBER |
| 8c. ADDRESS (City, State, and ZIP Code)<br>Washington, DC 20362-5101 | 10. SOURCE OF FUNDING NUMBERS<br>PROGRAM ELEMENT NO. 62712N; PROJECT NO. RS12-131 001; TASK NO; WORK UNIT ACCESSION NO DN155-014 |
| 11. TITLE (Include Security Classification)<br>Phase Pattern of Phased Array Element | |
| 12. PERSONAL AUTHOR(S)<br>Rao, J.B.L. and Cheston, T.C. | |
| 13a. TYPE OF REPORT<br>Interim<br>13b. TIME COVERED FROM _____ TO _____ | 14. DATE OF REPORT (Year, Month, Day)<br>1986 December 31<br>15. PAGE COUNT<br>17 |
| 16. SUPPLEMENTARY NOTATION | |

| 17. COSATI CODES | | |
|---|---|---|
| FIELD | GROUP | SUB-GROUP |
| | | |
| | | |

18. SUBJECT TERMS (Continue on reverse if necessary and identify by block number)
Phased pattern, Non-planar phase front
Phased array Element pattern

19. ABSTRACT (Continue on reverse if necessary and identify by block number)

The radiation-phase-pattern of a phased array element was measured to assess performance when used in an array requiring a non-planar phasefront. The E- and H-plane element-phase-patterns were found to give constant phase for scan-angles exceeding 60°, but the phase centers were displaced from each other. This separation has to be taken into account when calculating required phase settings for non-planar aperture excitations.

| | |
|---|---|
| 20. DISTRIBUTION/AVAILABILITY OF ABSTRACT<br>☐ UNCLASSIFIED/UNLIMITED ☒ SAME AS RPT ☐ DTIC USERS | 21. ABSTRACT SECURITY CLASSIFICATION<br>UNCLASSIFIED |
| 22a. NAME OF RESPONSIBLE INDIVIDUAL<br>J.B.L. Rao | 22b. TELEPHONE (Include Area Code)<br>(202) 767-2584<br>22c. OFFICE SYMBOL<br>Code 5372 |

DD FORM 1473, 84 MAR 83 APR edition may be used until exhausted
All other editions are obsolete

SECURITY CLASSIFICATION OF THIS PAGE

GU.S. Government Printing Office: 1985-607-047

CONTENTS



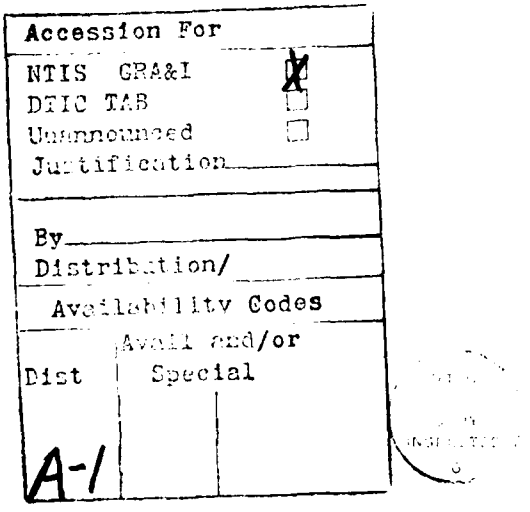

# PHASE PATTERN OF PHASED ARRAY ELEMENT

## INTRODUCTION

The radiation pattern of a phased array composed of equally spaced similar radiating elements is the product of the array factor and the element pattern [1]. The scanned antenna gain follows the element pattern which is, therefore, of considerable interest in determining the characteristics of a phased array.

The element pattern of an array can be measured to assure proper performance by measuring the pattern of one element when surrounded by many others that are resistively terminated. All elements are assumed equal and edge effects are neglected. When perfectly matched, the element power radiation pattern is of the form cos θ since the total power incident on the aperture varies as cos θ. Deviations from that value are due to aperture mismatch, i.e., to the reflection coefficient Γ, and grating lobes. Hannan [2] showed that when the array lattice spacing is such that grating lobes do not appear within the portion of the visible region, then element power pattern in the terminated array environment is

$$P(\theta,\phi) = \frac{D_x D_y}{\lambda^2} \left(1 - |\Gamma(\theta,\phi)|^2\right)\cos\theta \qquad (1)$$

where $D_x$ and $D_y$ represent inter-element spacings and $\Gamma(\theta,\phi)$ = active voltage reflection coefficient.

Manuscript approved October 8, 1986.

Equation (1) provides the relation between the active element amplitude pattern and the aperture mismatch (denoted by the reflection coefficient) but does not provide information on the phase of the element pattern. An alternate equation gives the active element voltage pattern as [3].

$$F(\theta,\phi) = \frac{Z_o + Z_g}{2R_g} F^o(\theta,\phi)[1 - \Gamma(\theta,\phi)] \qquad (2)$$

where $Z_g$ is the internal impedance of the driving generators ($R_g$=Real part of $Z_g$),

$Z_o$ is the input impedance of an element in the open circuited array environment

and $F^o(\theta,\phi)$ is the element pattern function in the open-circuited array environment.

In general, $F^o(\theta,\phi)$ is complex and the element pattern phase depends not only on mismatch (hence $\Gamma$) but also on $F^o(\theta,\phi)$. For a simple element like a dipole, $F^o(\theta,\phi)$ can be assumed to be a real function [4] and eq. (2) can be rewritten as

$$F(\theta,\phi) = K\,[1 - \Gamma(\theta,\phi)] \qquad (3)$$

where K is a constant.

The reflection coefficient varies with scan angle and can introduce a maximum phase change $\phi_m$ given by

$$\phi_m = \sin^{-1}|\Gamma(\theta,\phi)| = \sin^{-1}\frac{VSWR - 1}{VSWR + 1} \qquad (4)$$

as illustrated in Fig. 1. As an example, if the VSWR=2, then the corresponding magnitude of the reflection coefficient is 0.33 and the element pattern phase change can be as high as ±19°.

The reflection coefficient typically varies considerably with scanning and corresponds to the change of aperture impedance.

The phase of the element radiation pattern, in addition to its amplitude, becomes important when an array is used with a non-planar phase distribution. For example, a phased array aperture distribution may include a spherical phase front in order to focus when a phased array is used as a lens. It is also required when the aperture is focussed on a monitor to check the performance of individual elements which are sequentially phase-modulated, or to check the radiation pattern by scanning past the monitor. Further, phase perturbations may be introduced to generate multiple beams or to shape the radiation pattern. Under all of these conditions of non-uniform phase front, the individual element phase and amplitude patterns are used with varying look-angles $\theta$. This is most easily seen in the case of a phased array focussed to a central point. For a central element $\theta=0$ but an edge element has a look-angle $\theta=\tan^{-1}\frac{a}{2f}$ (a = aperture size, f = focal length).

**MEASURED PHASE PATTERN**

A previously developed 121 element aperture was used to measure the phase pattern. Figure 2 shows the experimental array which was built for a previous program and found to be reasonably broadband with a VSWR of about 2:1 over a frequency range of 2.8 to 4.2 GHz and over the scan range of ±60°. The array consisted of parallel plate waveguides with rectangular strip probes fed by coaxial lines. Figure 3 gives details of the probe design and the feeding arrangement. Figure 4 shows the test set up used for phase measurement of the center element (probe) when all the

other elements are terminated in matched loads (50Ω ). The array phase center, which gives minimum phase variation, is obtained by trial and error. The phase center was found to be stationary over the whole 40% band. For the H-plane, the phase center was found to be about 0.112" behind the probe and almost 1.112" inside from the septa edges, as shown in the insert of Fig. 5. Figure 5 shows the H-plane phase pattern at 3.2 GHz. The phase remained fairly constant, over an angle of more than ±60°; random variation amounted to about ±4°. Figure 6 shows the H-plane phase pattern vs angle at 4.0 GHz. Again, the phase remained fairly constant except for a random variation of about ±4° over ±60°. The random variations are attributed to experimental errors.

For the E-plane pattern, the center of phase was found to be midway in the mouth of the septa, as illustrated in Fig. 7 which also shows the E-plane phase pattern at 3.2 GHz. Figure 8 shows the E-plane phase pattern vs angle at 4 GHz. These results show that the E-plane radiation pattern phase also remained fairly constant over an angle of ±60°, except for random variations of about ±4°.

When scanning in the combined plane, both results have to be taken into account. Cylindrical spreading occurs first in the H-plane starting close to the element followed by scanning in the E-plane when the mouth of the septa is reached.

**CONCLUSIONS**

Theoretical analysis predicted the possibility of a change in phase of the element radiation pattern when there is a change in phased array aperture match condition, and hence, with scan angle. However, the experimental results presented in this report reveal that the E- and H-plane element-phase-patterns give constant phase for scan angles up to,

and exceeding, 60°. The E- and H-plane phase centers were found to be displaced from each other which has to be taken into account when calculating phase settings for non-planar aperture excitations.

## REFERENCES


1. Skolnik, M.I., RADAR HANDBOOK, New York, McGraw-Hill, 1970, pp. 11-23.

2. Hannan, P.W., "The Element-Gain Paradox for a Phased-Array Antenna," IEEE Trans. Antennas and Propagation, Vol. AP-12, pp. 423-433, 1964.

3. Wasylkiwskyj, W. and Kahn, W.K., "Element Patterns and Active Reflection Coefficient in Uniform Phased Arrays," IEEE Trans. Antennas and Propagation, Vol. AP-22, pp. 207-212, 1974.

4. Kahn, W.K., Private communication.

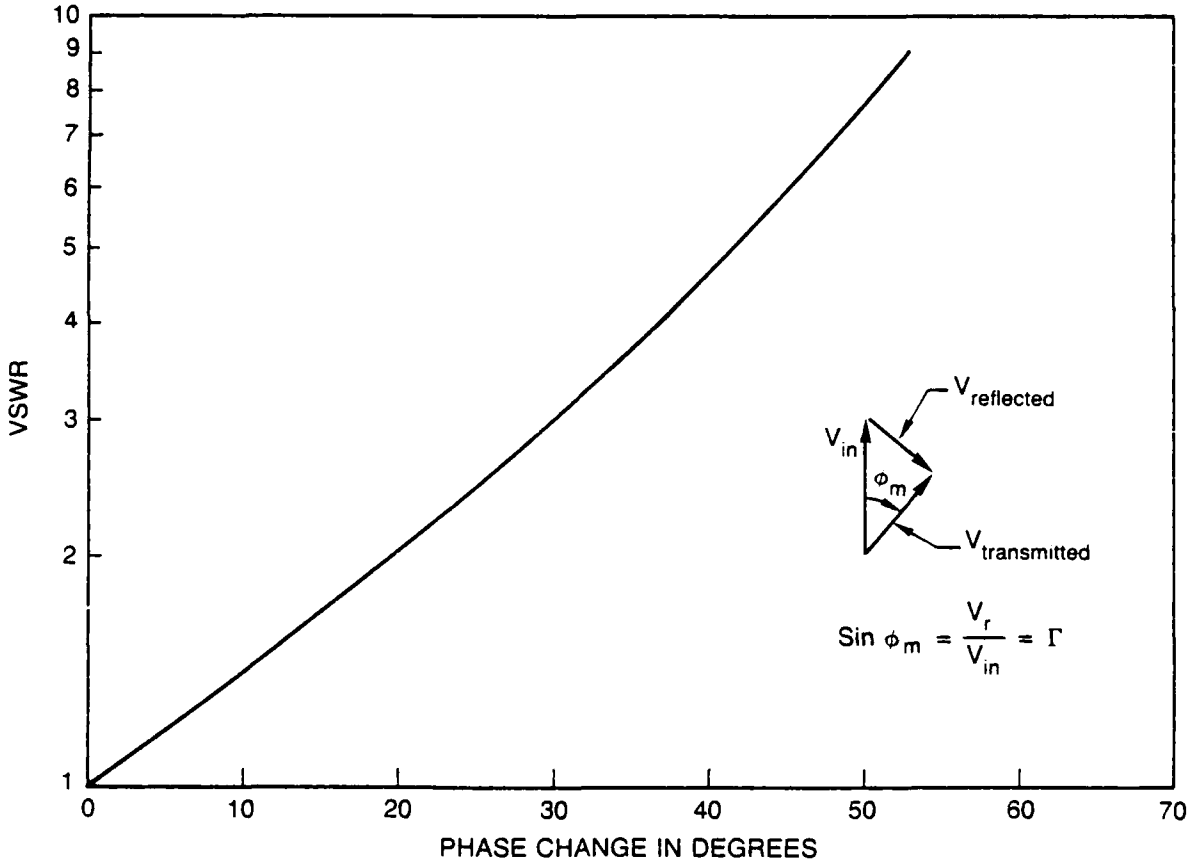


Fig. 1 — Maximum possible change in transmission phase due to a single reflection coefficient Γ

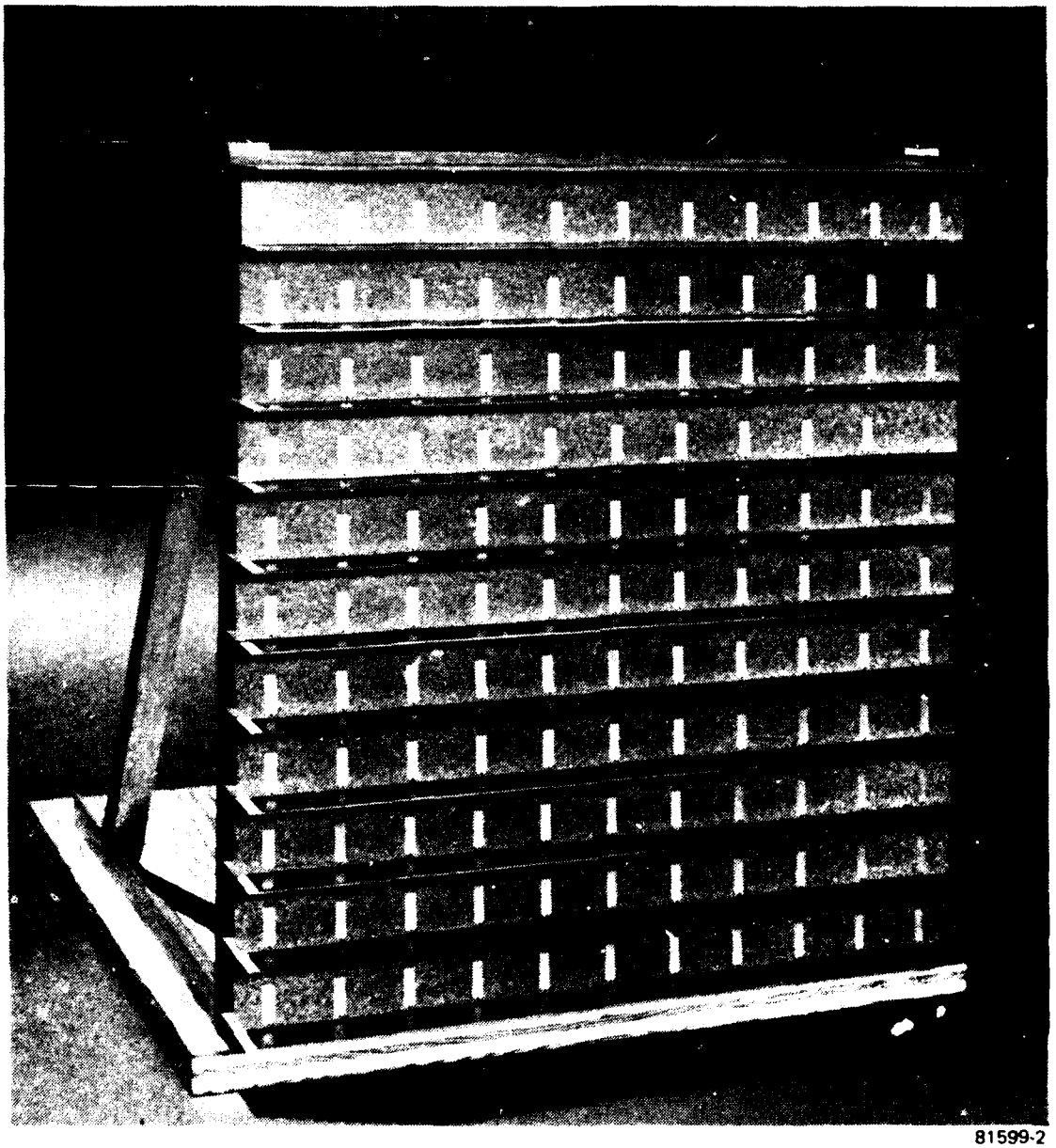

81599-2

Fig. 2 — Actual experiment array

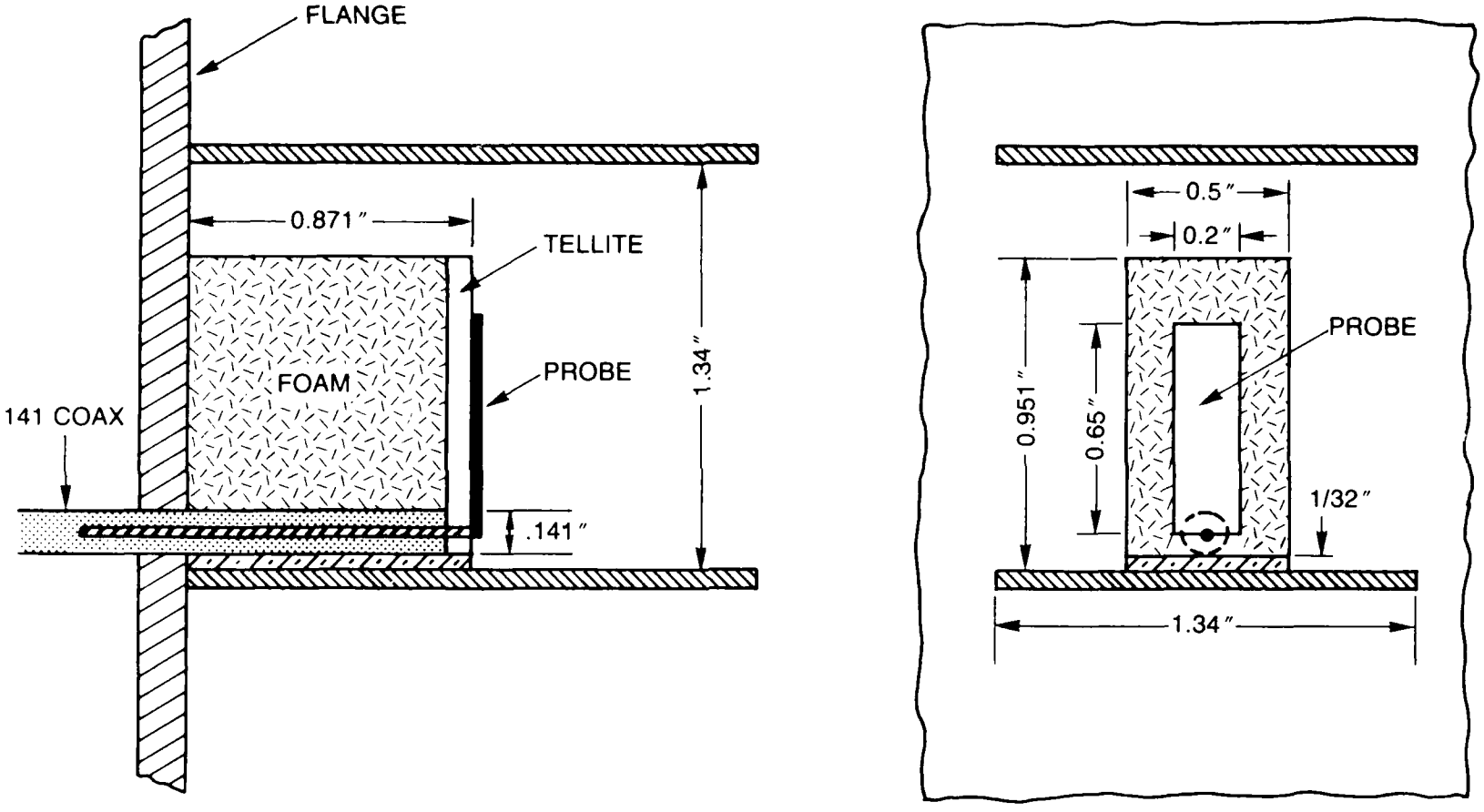


Fig. 3 — Detail geometry of the end-on bottom fed probe

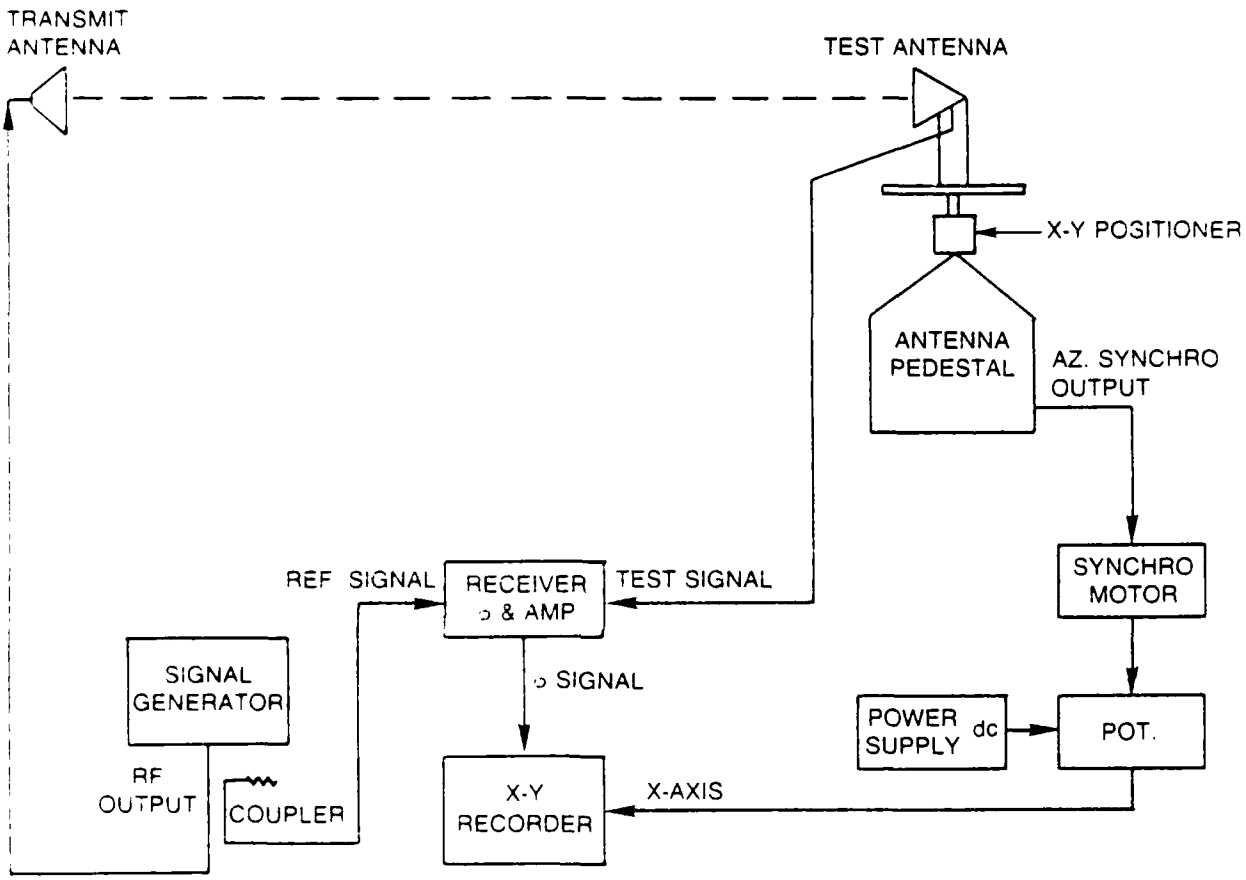


Fig. 4 — Test set up for measuring phase pattern of phased array element

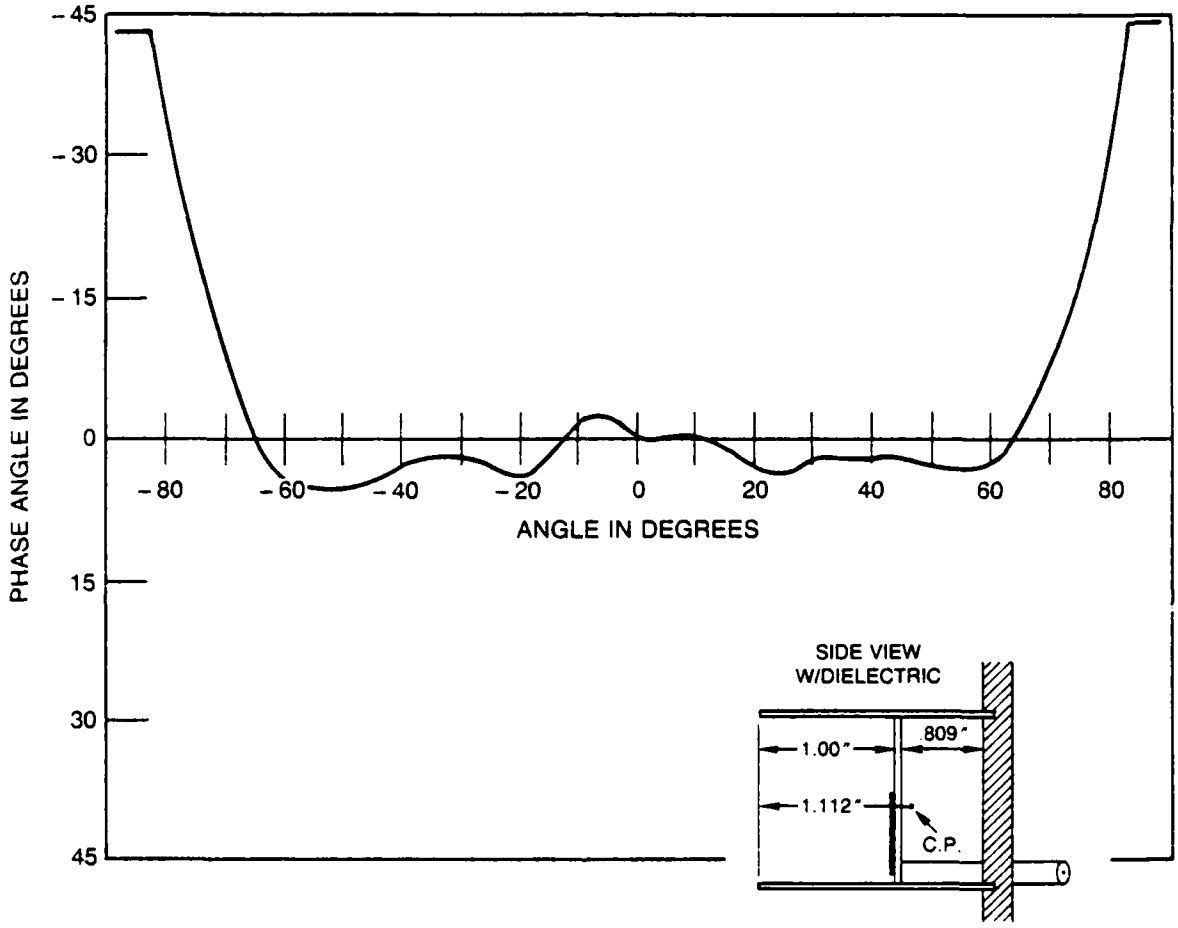


Fig. 5 — H-plane phase pattern, $F$ = 3.2 GHz

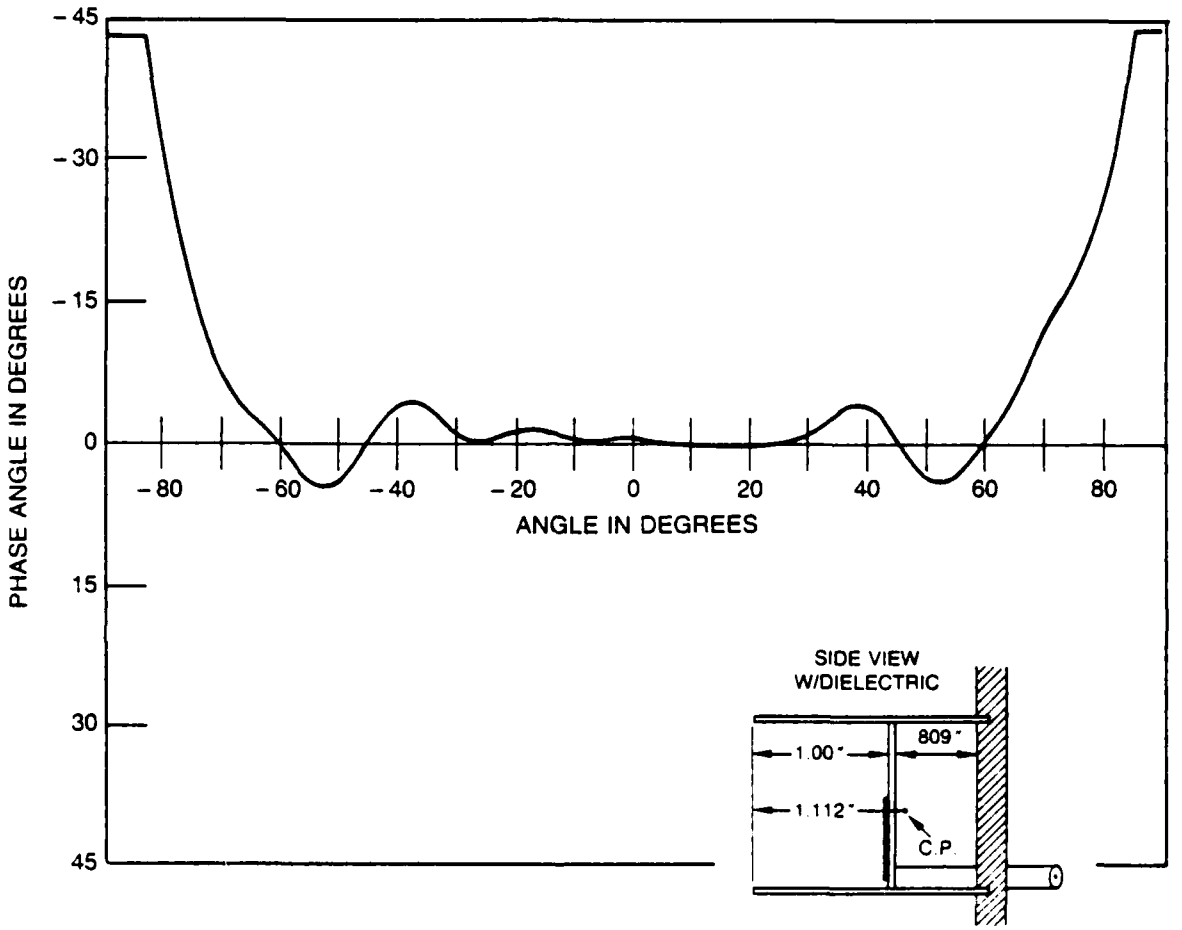


Fig. 6 — H-plane phase pattern, $F = 4$ GHz

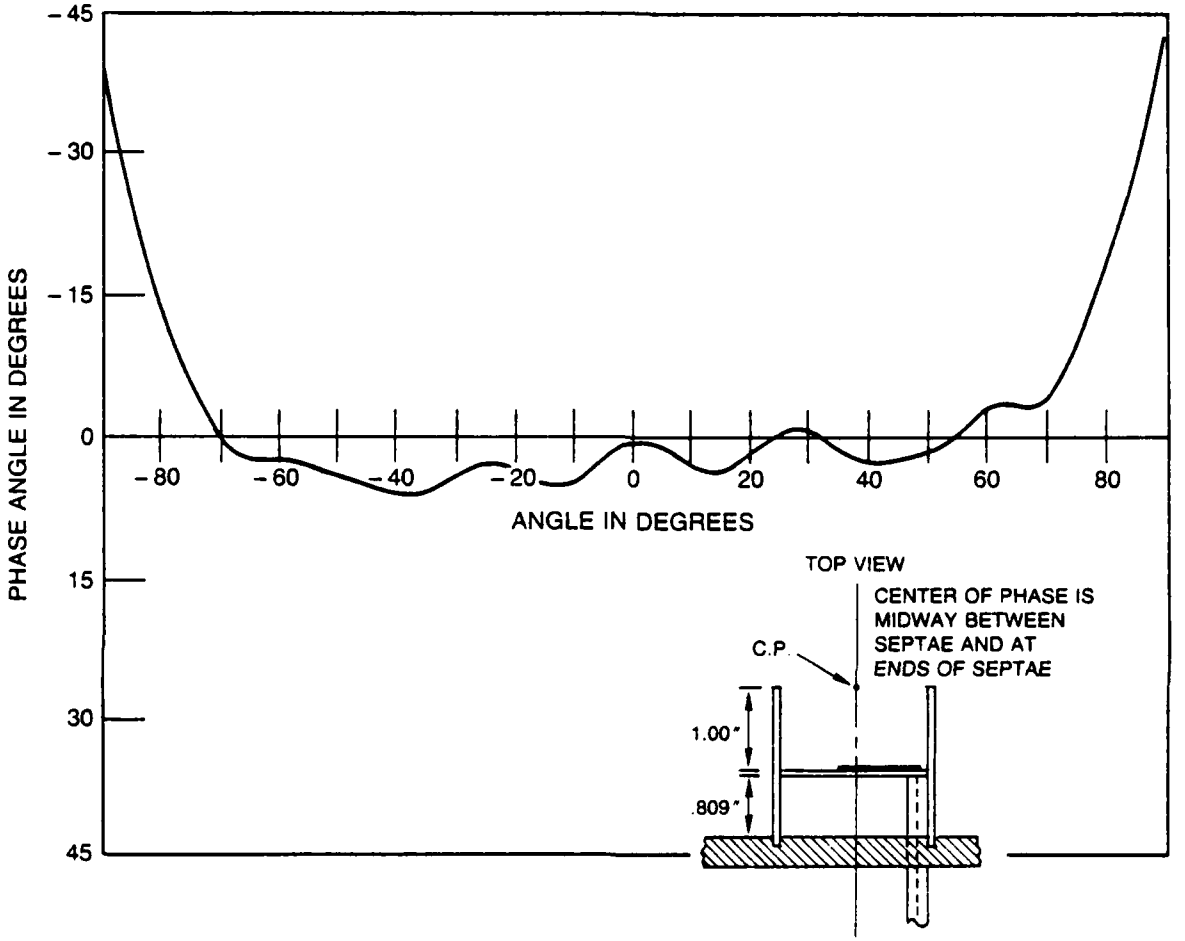


Fig. 7 — E-plane phase pattern, $F = 3.2$ GHz

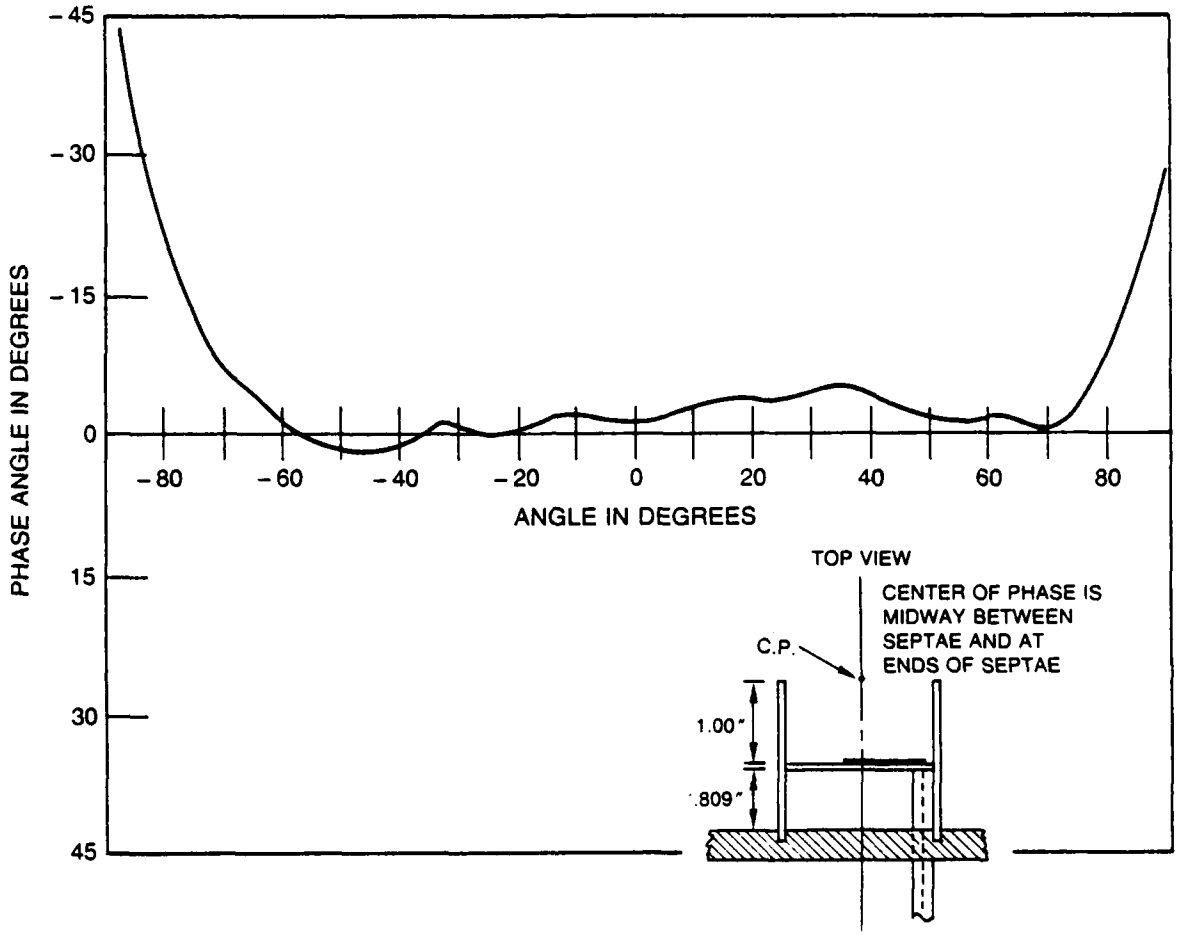


Fig. 8 — E-plane phase pattern, $F = 4$ GHz

END

3-87

DTIC